EasyChair Preprint

№ 14661

# ED-Net: Unified Enhancement-Denoising Deep Convolutional Network for Low-Light Mining Images

Jiaqi Wu, Da Lu, Yu Tao, Hui Ding and Guoping Huo



September 3, 2024

# ED-Net: Unified Enhancement-Denoising Deep Convolutional Network for Low-Light Mining Images

Jiaqi Wu[1][0009−0002−0864−2529], Da Lu[1][0009−0006−5641−233X], Yu Tao[1][0009−0007−4479−3785], Hui Ding[1][0000−0002−1920−7613](✉), and Guoping Huo[2][0009−0006−4504−8149](✉)

[1] College of Information Engineering, Capital Normal University, Beijing, China
dhui@cnu.edu.cn
[2] School of Artificial Intelligence, China University of Mining and Technology-Beijing, China
kuoping@cumtb.edu.cn

**Abstract.** The mining environment poses unique challenges for image processing due to low illumination conditions and the presence of various types of noise. Existing image enhancement methods typically focus on either brightness enhancement or noise reduction, but rarely address both issues simultaneously. This paper proposes ED-Net, a unified model that simultaneously tackles both brightness enhancement and noise reduction through a novel joint loss function design. Addressing the lack of open-source mining image datasets, the authors introduce a method for constructing a low-illumination noise dataset to simulate the mining environment. Evaluated on the BSDS500 dataset, ED-Net demonstrates superior performance compared to state-of-the-art algorithms in terms of PSNR, SSIM, VIF metrics, and visual quality. The key innovations lie in the unified brightness enhancement and noise reduction model, the effective joint loss function, and the low-illumination noise dataset construction method for simulating mining images.

**Keywords:** Mine Image Enhancement · Image Denoising · Histogram Matching · Deep Convolution · Loss Function.

## 1 Intruduction

Advanced image processing and data analysis play a crucial role in the mining industry during the digital era. Nevertheless, the distinctive attributes of these environments, such as limited illumination, particulate matter, and airborne particles, present considerable obstacles to image processing. Consequently, it often leads to images with poor contrast, lack of sharpness, and excessive noise, thereby impeding environmental monitoring, increasing the likelihood of accidents, and reducing operational effectiveness.

Recent advancements in image denoising include several notable approaches. Lehtinen et al.[1] demonstrated learning image restoration from corrupted examples, often surpassing clean data-trained models. Krull et al.[2] extended this

with Noise2Void (N2V) for independent noisy image pairs. Niu et al.[3] introduced Noise2Sim, a nonlocal, nonlinear self-supervised denoising method. Kulikov et al.[4] developed SinDDM, a denoising diffusion model improving image generation, editing, and restoration. Gong et al.[5] highlighted DDPM-based methods' effectiveness for PET image denoising. Yan et al. [6] proposed regularization to address overparameterization and overfitting in denoising models.

In image enhancement, Guo et al.[7] and Li et al.[8] proposed Zero-Reference Deep Curve Estimation (Zero-DCE) for low-light enhancement without training data. Su et al.[9] applied zero-reference deep learning for 3D reconstruction of underground utilities. The Self-Calibrated Illumination (SCI) framework [10] was developed for efficient and robust image brightening in low-light conditions. A multi-algorithm strategy is often needed to handle complex environments efficiently.

Since most of the noise in the mine is multiplicative, and it also has Gaussian noise caused by dust and dust in the environment. Mining images tend to be more special. Furthermore, it is difficult to photograph during production, there are no open-source datasets available for research. The construction of multiplicative noise models is also full of challenges. To address these issues, this paper proposed a unified enhancement-denoising deep convolutional network, our main contributions are as follows:

- **Unified Enhancement-Denoising, ED-Net**. To address the challenge of existing image enhancement methods not jointly considering brightness enhancement and noise reduction, we propose ED-Net, a CNN-based network that simultaneously performs brightness adjustment and denoising within its convolutional layers, effectively enhancing mining images.
- **Novel Loss Function Designed**. For low-illumination and noisy conditions, we introduce a joint loss function that integrates Mean Squared Error (MSE) [11] and the Structural Similarity Index Measure (SSIM) [12]. Additionally, considering edge preservation, we incorporate bilateral filtering [13].
- **Dataset Construction via Histogram Matching**. Conventional approaches for simulating low-illumination and noise rely on noise models, which may not accurately capture the complex conditions in mining environments with extremely low light and diverse noise types. We propose constructing a dataset by matching the histograms of real-world mining scenes, circumventing the need for noise models.

## 2 Related Work

### 2.1 Histogram Match

Histogram matching [14] is an image processing technique that aims to identify the pixel values in the reference image that have the same or closest probability as the original image. This is done by using the cumulative probability distribution map of the original image to establish a mapping relationship for each pixel. It can be characterized as:

$$s = T^{-1}(R(x, y)) \tag{1}$$

where $T^{-1}$ denotes the inverse transform function of the target image and $s$ is the gray level after matching.

By adjusting the gray scale distribution of the target image to resemble that of the mine image, we may achieve color or brightness correction between the photos. This allows us to match the images under varied lighting situations.

### 2.2 Noise2Noise Network

Noise2Noise [1] is a noise removal algorithm based on ground truth-free images as supervision. The fundamental concept is that with extended learning, the network may acquire the average value of all the distorted images by minimizing the loss function, thereby approximating the clean image.

For supervised training with clear images, the target image $y_i$ as well as his observed noise-containing image $\widehat{x_i}$, the use of the neural network to fit this regression model can be seen as optimizing an objective function:

$$arg\min_{\theta} \sum_{i} L(f_\theta(\widehat{x}_i), y_i) \tag{2}$$

$f_\theta$ is this neural network, and $\hat{x}$ can be viewed as the distribution of $x$ in terms of $y$, i.e., $\hat{x} \sim p(\hat{x}|y_i)$.

The Noise2Noise network has demonstrated excellent denoising capabilities. However, its performance can be adversely affected when dealing with images of poor quality. To address this limitation, the Noise2Clean approach can be employed, leveraging the Noise2Noise network as a baseline and introducing ground truth comparisons and constraints. By incorporating clean reference images, the Noise2Clean method can effectively handle a broader range of noisy and low-illumination scenarios, extending the applicability of the Noise2Noise network to scenarios where both noise and brightness levels are suboptimal.

The following optimization function is finally obtained:

$$arg\min_{\theta} \sum_{i} L(f_\theta(\widehat{x}_i), (\widehat{y}_i) \tag{3}$$

### 2.3 Zero-DCE Network

The Zero-DCE [7] (Zero-Reference Deep Curve Estimation) algorithm is a deep learning technique used for enhancing images. The main concept is to train a deep neural network to learn curve properties in an image, such as contrast and brightness, without using a reference image. These curve features are then used to enhance the image.

Inspired by the luminance adjustment curve in Photoshop, the author tried to design a curve that automatically maps a low-light image to an enhanced

version, and the parameters of the adaptive curve are only related to the input image.

The Luminance Enhancement Curve (LE-curve) formula is as follows:

$$LE(I(x);\alpha) = I(x) + \alpha I(x)(1 - I(x)) \tag{4}$$

Where $x$ denotes the pixel coordinates, $\alpha$ taking values in the range $[-1, 1]$, is a learnable parameter, $I(\mathbf{x})$ is the luminance value at the x-coordinate of the input image, and $LE(I(x);\alpha)$ is the luminance value after the brightening.

For brightness enhancement, zero-reference methods have demonstrated exceptional performance. However, in scenarios with extremely low illumination levels and without the availability of ground truth reference images, the performance of these methods can degrade. Consequently, in low-light conditions, it is beneficial to incorporate ground truth constraints to enhance the brightness enhancement capabilities of the network.

## 3 Methods

### 3.1 The architecture of ED-Net

Inspired by Noise2Noise and Zero-Reference Deep Curve Estimation (Zero-DCE) models, this paper proposes a Unified Enhancement Denoising Network, **ED-Net**. The proposed network adopts the Zero-DCE network as the fundamental framework and incorporates denoising processing within the convolutional layers. The overall network structure is illustrated in Fig.1.

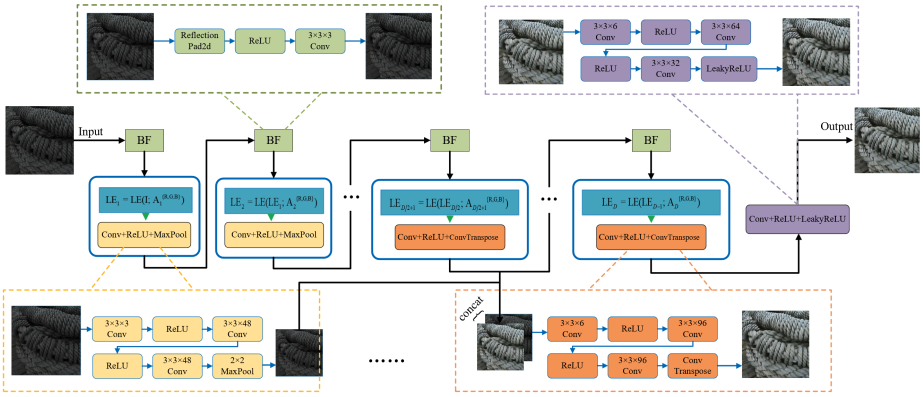


Fig. 1: The architecture of ED-Net.

The ED-Net is based on the Zero-DCE model, which learns to map a noisy low-light image input to a clean, brightness-enhanced target image. Due to the

extremely low brightness and high noise levels in underground mining images, we employed a supervised approach during the network processing, utilizing ground truth comparisons, specifically adopting Zero-Clean and Noise-Clean techniques.

In other words, given the challenging conditions of underground mining images with very low illumination and significant noise, the proposed ED-Net architecture is built upon the Zero-DCE model, which aims to transform noisy low-light input images into clean, brightness-enhanced target images. To achieve this, the network training process incorporates supervision by comparing the network outputs with ground truth clean target images, employing both Zero-Clean (mapping from zero-input to clean target) and Noise-Clean (mapping from noisy input to clean target) strategies.

The specific composition of the ED-Net network is: (i) Conv+ReLU+MaxPool: for layers $1 \sim (D/2)$ , a color image of size 128 $\times$ 128 is used as input, 48 filters of size 3 $\times$ 3 $\times$ c are used to generate 48 feature maps, and then use the rectified linear unit ReLU for non-linearity. Finally, the number of channels is converted to 3 through 3 filters, the kernel size is 2 $\times$ 2, and the step size is 2 maximum pooling layer output. The variable c denotes the number of channels in an image, where c = 1 for grayscale images and c = 3 for color images. This method is a procedure of down-sampling. By preserving the primary characteristics of the original image, the feature map's size and parameter count are diminished, leading to enhanced computing efficiency and model generalization. (ii) Conv+ReLU+ConvTranspose: for layers $(D/2+1) \sim (D-1)$, similar to the previous method, this involves an upsampling procedure using three transposed convolutions with a kernel size of 3 x 3 and a step size of 2. The number of channels is classified as 3 and then output. (iii) Conv+ReLU+LeakyReLU: for the last layer, ReLU is applied with different numbers of filters using a 3x3 convolution kernel. To handle ReLU's zero output in the negative region, the last layer uses LeakyReLU as the output.

### 3.2 Innovative Loss Function

In the field of image enhancement, the loss function is crucial for evaluating model performance during training. Both Zero-DCE and Noise2Noise use a single loss function. Unlike Zero-DCE and Noise2Clean, we use a joint loss function for both brightness enhancement and noise removal.

Specifically, we opted to employ the amalgamation of Mean Squared Error (MSE) [11] and Structural Similarity Index Measure (SSIM) [12] to enhance the structural resemblance between the generated image and the target image, rather than solely focusing on the disparity at the pixel level. MSE is employed to quantify the precision of model predictions and facilitate optimization algorithms in identifying the optimal model parameters by minimizing the disparity between anticipated values and actual values. The formula is shown below:

$$MSE = \frac{1}{m}\sum_{i=1}^{m}(y_i - \widehat{y}_i)^2 \tag{5}$$

Where $y_i$ is the actual value, $\widehat{y}_i$ is the predicted. SSIM is a metric utilized to quantify the likeness between two photographs, taking into account three factors: brightness, contrast, and structure. As a result, it provides a more accurate representation of the image quality as experienced by people.

### 3.3 Dataset Construction

Deep learning models require a large amount of data for learning and training. Currently, many image enhancement datasets are open-source, such as BSD500, etc. However, there is a lack of open-source datasets for underground mine enhancement, as there is no way to obtain images with good brightness for the real environment undermines. Even in the shutdown state, the noise in the mine will decrease, but the brightness environment cannot be improved. When simulating degraded images, noise model simulation is typically used. However, this method often deviates greatly from reality.

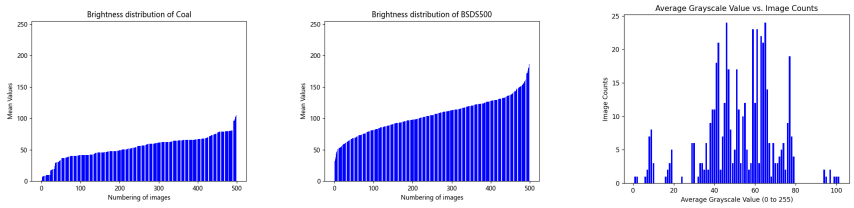


(a) (b) (c)

Fig. 2: Histograms of relevant statistics

**Low-light Images Generation** Based on the principle of histogram matching, we perform histogram matching on standard datasets, such as BSD500, that contain ground truth (with better illumination) similar to real mine images, thereby obtaining low-illumination images similar to the real situation. To make the constructed dataset closer to the real situation, we obtained 500 low-light images through the internet, news reports, and literature retrieval, and used random registration to construct a low-light dataset based on BSD500. Fig.2 presents relevant statistical histograms. The brightness distribution of the mean value of this dataset was calculated and plotted in (a). From Fig.2(a), we can observe that the majority of the images have an average brightness that falls within a range of 60 intervals. (b) presents the luminance distribution of the BSDS500 dataset, which has considerably higher mean values compared to the coal dataset. Furthermore, (c) presents the statistical data on the quantity of photographs within each brightness interval. This dataset constructed based on real environment image statistics has low illumination characteristics and will exhibit variations in different grayscale levels.

**Noise and Block Distortion Correction** The gray scale distribution of the real value image spans from 0 to 255, whereas the gray scale distribution of the dark image is more focused in the darker region compared to the true value image. As a consequence, there is a varied spectrum of grayscale distribution, and photographs that contain extensive patches of uniform color are susceptible to distortion while doing histogram matching. At first, we attempted to solely modify the saturation of the true-value image following histogram matching. However, the issue of distorted color blocks persists. Thus, it is imperative to conduct histogram matching using gray space and modify the range of the actual value image prior to completing histogram matching.

When constructing the dataset, preserving the original color integrity of the images is paramount. The RGB color space, responsible for color composition, is unsuitable for exclusive histogram matching due to potential nonlinear distortions. Therefore, we are exploring the use of the HSV color space. While histogram matching primarily adjusts the V channel, the S channel also influences color. To accommodate this, the saturation reduction parameter $\gamma$ can be tailored based on specific conditions. Subsequently, the luminance channel can establish the minimum and maximum values for histogram matching, thereby altering the grayscale distribution of dark images. However, this method overlooks the unique characteristics of authentic images and may result in distorted color blocks in regions of varying brightness. We also experimented with matching by averaging the lowest and highest values from the truth map and the dark image.

The required range of gray values $[\alpha, \beta]$ for the matched image was:

$$[\alpha, \beta] \in \left[\frac{1}{2}\left(\min_{\text{gt}}, \min_{\text{dark}}\right), \frac{1}{2}\left(\max_{\text{gt}}, \max_{\text{dark}}\right)\right]$$

Here are the Results of different histogram matching methods in Fig.3.

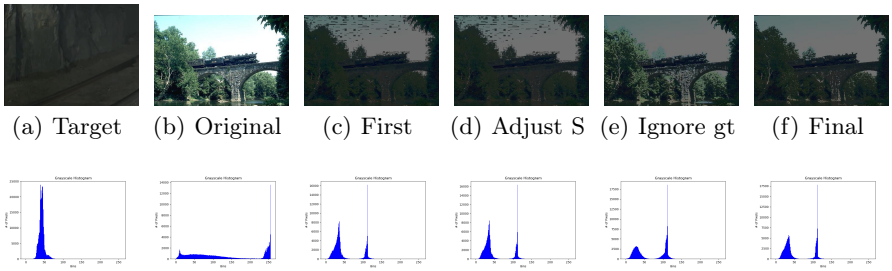

(a) Target (b) Original (c) First (d) Adjust S (e) Ignore gt (f) Final

(g) Hist of(a) (h) Hist of(b) (i) Hist of(c) (j) Hist of(d) (k) Hist of(e) (l) Hist of(f)

Fig. 3: Construction process of low illumination mine image

The adjustments made with this method produced smoother images, especially enhancing the processing of low-light images. However, even after multiple range adjustments, there were still challenges in processing the bright image of the ground truth. Further experiments revealed that the minimum value of the

grayscale range had less impact on the results, and the main problem was the insufficient grayscale range for its maximum value. Especially in extreme cases, overly bright images of the truth may need to be excluded.

To improve the accuracy of simulating image features in the mine environment, we applied a targeted noise enhancement method to the ground truth images before performing histogram matching preprocessing. To enhance the realism of the image simulation, we introduced Gaussian noise [15] with $\mu = 0$ and $\sigma = 0.08$ to the true value graph. Typically, the noise exhibits $\sigma$ within the range of 0.05 [16]. However, due to the complexity of the mine environment, it is adjusted to a higher value of 0.08. $\sigma$ will be further enhanced due to the alteration in low-light images following histogram matching.

This method is accomplished through the following steps: Initially, a noise template is created by introducing random noise within the range of pixel values from 0 to 255. This template is then normalized. Subsequently, the noise template is applied to each individual color channel of the image.

During the noise generation process, we only used Gaussian noise. This is because, although the underground mine environment contains various types of noise, especially multiplicative noise, our noise is added before reducing the brightness through histogram matching, which is consistent with the principle of multiplicative noise. Additionally, by using strong noise with $\sigma = 0.08$, this method better aligns with the mine environment.

## 4 Experiments

Our experimental environment consists of a Windows 10 Home China, 64-bit operating system running on a hardware configuration consisting of an Intel(R) Core(TM) i5-10210U CPU @ 1.60GHz 2.11 GHz with 16GB of RAM and an NVIDIA Python version 3.10.2 and CUDA version 11.6. During the studies, we maintained a uniform set of parameter values, including learning rate (lr) of 0.001, batch size of 4, and training for 100 epochs using the Adam optimizer.

### 4.1 Dataset and Metrics

To boost the quality of mining images, we adopted the methodology described in reference. We divided the training set and test set in the ratio of 8:2 and conducted training using a dataset of 400 images with $128 \times 128$ sizes which are from dataset BSDS500 [17]. We discovered that utilizing a larger training set only led to minimal enhancement. In order to train ED-Net for the purpose of denoising and enhancing specific types of noise with known noise levels, we focused on two distinct noise levels, namely $\sigma = 0.08$. For the test images, we used the remaining 100 images of the BSDS500 dataset for testing. The division of the training and testing sets is completely randomized.

This study employs six regularly utilized assessment metrics, Peak Signal-to-Noise Ratio (PSNR) [12], Structural Similarity Index (SSIM) [18], Mean Squared Error (MSE) [11], Visual Information Fidelity (VIF) [19], Image Fidelity Criterion (IFC) [20], and Naturalness Image Quality Evaluator (NIQE) [21].

### 4.2 Ablation Study

Multiple ablation experiments were conducted to demonstrate the effectiveness of each component in the loss function used for training the ED-Net. To ensure better preservation of edges and textural details, the proposed algorithm incorporates bilateral filtering within the convolutional implementation process. The

Table 1: On the datasets of this experiment, the quantitative results of five full-reference indicators including PSNR, SSIM, MSE, VIF and IFC, and one non-reference indicator NIQE.

| | Loss | | | Metrics | | | | | |
|---|---|---|---|---|---|---|---|---|---|
| | **L1** | **MSE** | **1-SSIM** | **PSNR↑** | **SSIM↑** | **MSE** | **VIF↑** | **IFC↑** | **NIQE↓** |
| **1** | ✓ | | | 28.0533 | 0.5872 | 1433.9656 | 0.0893 | 0.9354 | 27.3830 |
| **2** | | ✓ | | 28.0873 | 0.5930 | 1473.7472 | 0.0964 | 0.9398 | 26.9334 |
| **3** | ✓ | | ✓ | 28.0435 | 0.6170 | 2301.1288 | 0.1057 | 0.9422 | 22.3903 |
| **4** | | ✓ | ✓ | 28.1939 | 0.7018 | 1134.9839 | 0.1064 | 0.9494 | 21.3629 |
| **5** | ✓ | ✓ | | 28.0601 | 0.5815 | 1469.4012 | 0.0961 | 0.9423 | 25.1542 |
| **6** | ✓ | ✓ | ✓ | 28.0291 | 0.6220 | 1979.8175 | 0.0989 | 0.9306 | 24.7222 |

table 1 displays the outcomes of training different combinations of loss functions on ED-Net. Table 1 demonstrates that L1 loss is less effective than MSE loss when either L1 or MSE is employed as the loss function. This demonstrates the significance of Mean Squared Error (MSE) in accurately detecting and rectifying the noisy points in order to restore the image. Applying (1-SSIM) as a loss function preserves the structural information of the image from the beginning due to the rapid convergence of the SSIM loss. SSIM considers brightness, contrast, and structure, which effectively balances the different quality metrics during image enhancement and denoising, resulting in higher-quality processing outcomes. The table clearly demonstrates that the combination of MSE loss and SSIM consistently yields favorable outcomes across all the evaluation measures provided.

### 4.3 Comparative Experiments

To comprehensively evaluate the effectiveness of the proposed ED-Net, we conducted comparative analyses against several existing algorithms, including Zero-DCE, Noise2Noise, and SCI. For a fair comparison, we also included algorithms that utilize ground truth as a reference, such as Noise2Clean, Zero-Clean, and SCI-Clean, as shown in Table 2 and Fig.4.

From Fig.4, it is evident that the ED-Net algorithm outperforms the others in terms of color restoration, brightness enhancement, and edge preservation, particularly excelling in enhancing the platform area and detailed textures. Furthermore, as demonstrated in Table 2, the optimal result is highlighted in red font. ED-Net achieves superior performance across various metrics, including PSNR, SSIM, MSE, VIF, IFC, and NIQE, attaining optimal results among the compared algorithms.

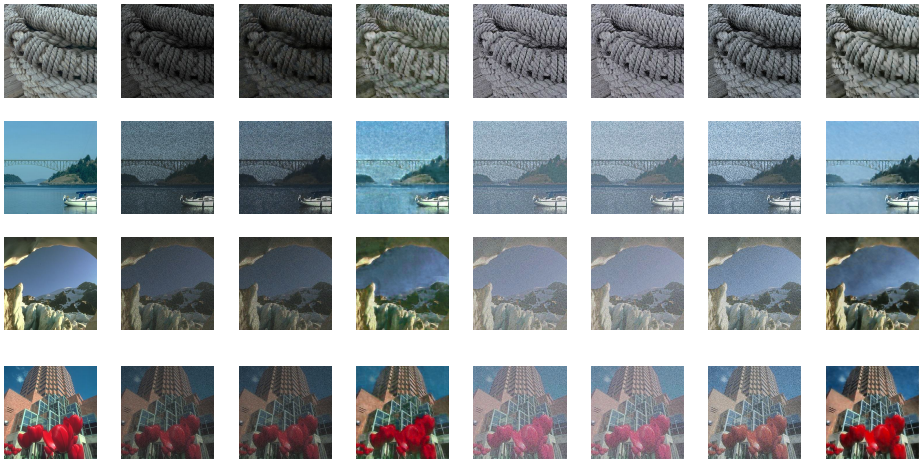

(a) GT (b) Dark (c) N2N (d) N2C (e) DCE (f) Z2C (g) SCI (h) ED

Fig. 4: Sample Images: Experimental Results of Different Algorithms

Table 2: Results of Comparison on Different Algorithms

| Methods | PSNR↑ | SSIM↑ | MSE↓ | VIF↑ | IFC↑ | NIQE↓ |
|---|---|---|---|---|---|---|
| **Noise2Noise,2019 [1]** | 27.9661 | 0.3559 | 5181.4467 | 0.1293 | 0.8988 | 14.2876 |
| **Zero-DCE,2020 [7]** | 27.8535 | 0.3879 | 3419.8502 | 0.0761 | 0.9257 | 13.3818 |
| **SCI,2022 [10]** | 27.9625 | 0.3682 | 5098.2715 | 0.1668 | 0.9046 | 13.0853 |
| **Noise2Clean** | 28.1914 | 0.6484 | 939.5286 | 0.0959 | 0.9399 | 27.0940 |
| **Zero-Clean** | 27.8556 | 0.3898 | 3408.4707 | 0.0766 | 0.9278 | 13.2645 |
| **SCI-Clean** | 27.9728 | 0.4013 | 3908.0817 | 0.1585 | 0.9307 | 13.6541 |
| **ED-Net** | 28.1939 | 0.7018 | 1134.9839 | 0.1064 | 0.9494 | 21.3629 |

### 4.4 Results of Real Mine Images

Furthermore, to assess the practical performance, we evaluated ED-Net on real underground mine images for experimental comparison. The test set comprised two images with a resolution of 640×480. During the testing process, instead of employing image cropping or scaling techniques, the entire image was directly used as input to obtain the predictions. The processing results are presented below.

As evident from Fig.5 showcasing the real images with noise, our proposed algorithm demonstrates superior performance in terms of brightness enhancement, color preservation, and preservation of intricate textural details when compared to the other methods. For the enhancement of images under low illumination and noise-containing pollution in the mine, it can be seen that the ED-Net has the best results in terms of visual effects in terms of overall brightness enhancement, and the degree of color retention, especially in terms of texture detail.

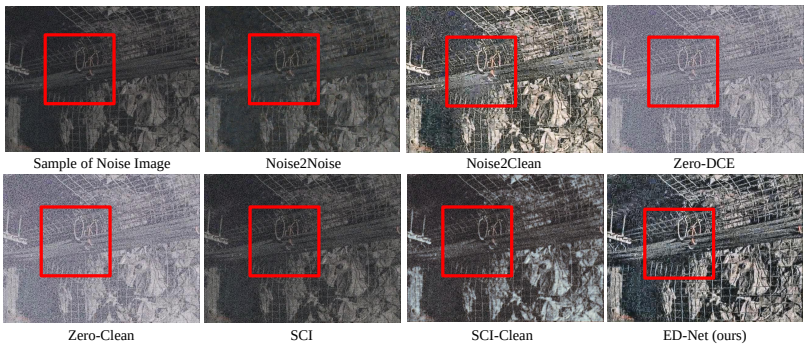


Fig. 5: Comparison on Real Sample Images and Noise Sample Images.

## 5 Conclusions

In addressing the dual challenges of low illumination and complex noise in underground mining images, we introduce ED-Net, an advanced network based on the zero-DCE model for concurrent brightness enhancement and denoising. The method leverages a novel histogram matching-based simulation to generate realistic mine images under varied conditions, reflecting the multiplicative noise characteristics of actual mining environments. Utilizing the BSD500 dataset, a specialized low-light noise dataset was created to accurately represent these challenging conditions. The deeply coupled convolutional architecture of ED-Net facilitates seamless integration of brightness adjustment and noise reduction, supported by a joint loss function that mitigates color block effects in flat areas, ensuring detail preservation and undistorted colors.

Comprehensive experiments on the BSDS500 dataset validate the superior performance of ED-Net, showcasing its capability to effectively process noisy, low-light mine images. The network excels in brightness enhancement, color fidelity, and texture detail preservation, surpassing existing methods. The resultant images maintain their integrity without distortion, providing a robust foundation for further analysis and enhancing the overall safety and efficiency of mining operations.

## References

1. Lehtinen, J., Munkberg, J., Hasselgren, J., Laine, S., Karras, T., Aittala, M., Aila, T.: Noise2Noise: Learning Image Restoration Without Clean Data. In: IEEE Conference on Computer Vision and Pattern Recognition (2019)
2. Krull, A., Vicar, T., Jug, F.: Probabilistic Noise2Void: Unsupervised Content-Aware Denoising. In: SCI (2020)
3. Niu, C., Li, M., Fan, F., Wu, W., Guo, X., Lyu, Q., Wang, G.: Noise Suppression With Similarity-Based Self-Supervised Deep Learning. IEEE Transactions on Medical Imaging (2023)

4. Kulikov, V., Yadin, S., Kleiner, M., Michaeli, T.: SinDDM: A Single Image Denoising Diffusion Model. In: ICML (2023)
5. Gong, K., Johnson, K., El Fakhri, G., Li, Q., Pan, T.: PET Image Denoising Based on Denoising Diffusion Probabilistic Model. European Journal of Nuclear Medicine and Molecular Imaging Journal **2**(5), 358–368 (2024)
6. Yan, Z., Liu, Z., Li, J.: Boosting of Implicit Neural Representation-based Image Denoiser. In: ARXIV-CS.CV (2024)
7. Guo, C., Li, C., Guo, J., Loy, C.C., Hou, J., Kwong, S., Cong, R.: Zero-Reference Deep Curve Estimation for Low-Light Image Enhancement. In: IEEE Conference on Computer Vision and Pattern Recognition (2020)
8. Li, C., Guo, C., Loy, C.C.: Learning to Enhance Low-Light Image Via Zero-Reference Deep Curve Estimation. IEEE Transactions on Pattern Analysis and Machine Intelligence (2022)
9. Su, Y., Wang, J., Wang, X., Hu, L., Yao, Y., Shou, W., Li, D.: Zero-reference Deep Learning for Low-light Image Enhancement of Underground Utilities 3D Reconstruction. Automation in Construction (2023)
10. Ma, L., Ma, T., Liu, R., Fan, X., Luo, Z.: Toward Fast, Flexible, and Robust Low-Light Image Enhancement. In: IEEE Conference on Computer Vision and Pattern Recognition (2022)
11. Allen, D.M.: Mean Square Error of Prediction As A Criterion for Selecting Variables. Technometrics (1971)
12. Sara, U., Akter, M., Uddin, M.S.: Image Quality Assessment Through FSIM, SSIM, MSE and PSNR—A Comparative Study. Journal of Computer and Communications (2019)
13. Tomasi, C., Manduchi, R.: Bilateral Filtering For Gray And Color Images. In: ICCV (1998)
14. Zhang, Y., Li, M., Li, R., Jia, K., Zhang, L.: Exact Feature Distribution Matching for Arbitrary Style Transfer and Domain Generalization (2022)
15. Chabanov, A.A.: Statistics of Random Signal Intensity in The Presence of Gaussian Noise. In: Frontiers in Optics (2007)
16. Zhang, K., Zuo, W., Chen, Y., Meng, D., Zhang, L.: Beyond a Gaussian Denoiser: Residual Learning of Deep CNN for Image Denoising. IEEE (2019)
17. Martin, D., Fowlkes, C., Tal, D., et al.: A Database of Human Segmented Natural Images and Its Application to Evaluating Segmentation Algorithms and Measuring Ecological Statistics. In: Proceedings of the Eighth IEEE International Conference on Computer Vision, ICCV 2001, 2:416-423.
18. Wang, Z., Bovik, A.C., Sheikh, H.R., et al.: Image Quality Assessment: From Error Visibility to Structural Similarity. IEEE Transactions on Image Processing **13**(4), 600–612 (2004)
19. Han, Y., Cai, Y., Cao, Y., Xu, X.: A New Image Fusion Performance Metric Based on Visual Information Fidelity. Information Fusion (2013)
20. Sheikh, H.R., Bovik, A.C., de Veciana, G.: An Information Fidelity Criterion for Image Quality Assessment Using Natural Scene Statistics. IEEE Transactions on Image Processing (2005)
21. Mittal, A., Soundararajan, R., Bovik, A.: Making A "Completely Blind" Image Quality Analyzer. IEEE Signal Processing Letters (2013)